

# Effects of Real Instrument on Performance of an Energy Detection-Based Spectrum Sensing Method

D. Capriglione, IEEE Member, G. Cerro, IEEE Member, L. Ferrigno, IEEE Member, G. Miele, IEEE Member

**Abstract**—In Cognitive Radio networks the role of spectrum sensing is crucial to efficiently exploit the radio spectrum resource and avoid harmful interference to legacy users. The need to measure spectrum occupancy turns Cognitive Radios to be *de facto* measurement instruments. This issue pushes the measurement community to analyze their behavior and to remark how real instrumentation problems could negatively affect performance in spectral measurements, thus provoking a poor-quality spectrum sensing outcomings. In particular, Software Defined Radios are adopted in this paper as cognitive devices, and their capability to accurately measure spectrum components is analyzed in comparison with a simulation set-up, where the same Analog-to-Digital Converter is modeled and simulated, and equivalent Signal-to-Noise Ratios are replicated. The final aim is to prove how nominal Signal-to-Noise ratio is not sufficient to model the impairments of a real acquisition, even jointly with an accurate modeling of the digitalization process. Compared results show an appreciable mismatch between simulation and real hardware acquisition and processing.

**Index Terms**— frequency-domain analysis, measurement, software radio, cognitive radio, analog-digital conversion.

## I. INTRODUCTION

Dynamic spectrum access (DSA) is one of the keywords for modern wireless networks and multimedia mobile applications [1], [2]. The traditional frequency allocation policy divides the radio spectrum resource in several frequency intervals and assigns each frequency interval to a specific communication technology. Usually each country divides each frequency interval in several sub-bands and each of them assigned to a user (licensee) that has the right to exploit that resource. This is done without any consideration about the actual occupancy of such band in a given time interval. Of course, this solution is not efficient in all situations when the licensee uses the spectrum for only a small portion of the time [3]-[4].

DSA, in compliance with the today telecommunication needs [4], gives the possibility to consider the spectrum occupancy as a dynamic solution, exploiting frequency bands that are allocated for specified services and not currently used by their licensed users. In detail, DSA allows novel approaches [5],[6] to make the cited applications suitably deployed and not in contrast with the scarce spectrum availability caused by traditional frequency allocation policies that have brought to a

non-optimized use of the radio spectrum resource.

To face issues provided by DSA new international regulatory and technical committees are proposing new standards and boundaries for the spectrum access.

For example, in the TV White Spaces (TVWSs) context, several standards are being developed to exploit the spectrum holes left free by TV broadcasters in Very High Frequency (VHF) and Ultra High Frequency (UHF) bands. In this context, the IEEE 802.22 standard [7] specifies MAC and PHY layers of a Wireless Regional Area Network (WRAN) that operates in VHF and UHF bands to reach a maximum data rate close to 23 Mbit/s and coverage area with a radius of 30 km with a single BS.

New hardware devices, namely the Cognitive Radios (CRs) can solve the DSA and regulatory issues since their ability to sense spectrum use by neighboring users (Primary Users or PUs) and to change dynamically their transmitting parameters (carrier frequency, bandwidth, modulation scheme) when a PU is starting to occupy its bandwidth, or a better spectrum opportunity is found [8]-[11]. To accomplish for all these tasks, CRs typically adopt Software Defined Radios (SDRs), which are devices in which their transmitting and receiving chains can be configured via software. SDRs allow great flexibility and could dynamically adjust all their parameters to take into account changes in the operating scenario [12]. Considering the receiving chain of SDR, it generally includes several stages among which: (i) an analog wideband radio frequency front-end equipped with circuitry and a mixer for a down-frequency conversion, (ii) input bank of filters for the selection of the operating frequency range, (iii) analog to-digital converters for signal acquisition and (iv) finite arithmetic-based processing units. The core of this last unit, (iv), is the execution of the spectrum sensing (SS) task. This task identifies the portions of radio spectrum that are not currently in use, often also known as frequency holes.

Even if many digital algorithms belonging to informed and uninformed (blind) techniques [13]-[16] are present in literature, new SS methods are today designed and developed with the aims of satisfying new issues proposed by DSA. Some important and often contrasting requirements, as (i) the capability of detecting the presence of PUs also with unfavorable SNR, (ii) the promptness in detecting a PU which starts to occupy the channel previously left free, (iii) the capability of measuring with good accuracy and resolution the

frequency range occupied by PUs. These new issues impose to verify the efficiency and the reliability of these algorithms respect to these new requirements.

In most cases the performance of spectrum sensing methods is evaluated in simulation environments on the basis of theoretical models and they are analyzed by considering mainly the non-idealities of the communication channel [17]-[21]. Only the quantization due to the ADC process is sometimes considered.

On the contrary, the typical receiving chain of an SDR is composed by several nonlinear components that could influence the overall performance of the SS stage as well. For instance, some papers have shown that radio front-end amplifier nonlinearities on both energy and cyclostationarity based SSs worsen the detection performance since it is dependent on the modulation types of the blockers and the signal of interest [22].

Considering these peculiarities of SDRs architectures and the needs of characterizing the SS expected performance, a new problem arises: “are the typical performance evaluation methods adopted to test SS algorithms, based only to the imposing of different SNRs, reliable for these kinds of applications?”.

This paper, starting from a preliminary simulation study on the effect of the ADC vertical resolution on the performance of spectrum sensing techniques carried out in [23] and stemming from the experience of the authors in system characterization [24], tries to give an answer to this problem for the special context of SDR devices, comparing performance characterizations of a typical SS method based on the energy detection [16], [25], in simulated and real scenarios. The aim of the paper is twofold: a) to show that a simulation approach that considers only the quantization noise and imposed SNRs is not sufficient to predict achievable performance of SS algorithms when implemented in SDRs; b) identify and modelling the non-linear device, involved in the SDRs Rx chain, to define reliable simulation scenarios to characterize SDRs performance.

The paper is then structured as follows: in Section II a state of the art in the field of performance assessment criteria for spectrum sensing techniques is proposed; Section III gives important details about the Rx chain of Software Defined Radio; in Section IV our adopted test methodology, consisting of a preliminary characterization of the device under test and a subsequent test phase with controlled scenario, is illustrated; performance assessment and comparison between simulation and real hardware results are reported in Section V. Conclusions follow in Section VI.

## II. RELATED WORKS

Generally, papers present in literature mainly focus their attention on the performance evaluation of proposed methods analyzing some figures of merit that quantify the probability of detection and the false alarm probability. To this aim, both theoretical and numeric/experimental tests are adopted. Such figures of merit are evaluated for different power level of the PU to be detected or for different SNRs. As an example, in [17] the performance of the spectrum sensing method proposed by the authors is evaluated by analyzing the probability of

detection and the probability of missed detection (for a given probability of false alarm) as a function of the PU signal power. The non-idealities of the receiving chain are neither modeled nor taken into account.

In [18], the performance analysis of the proposed Bayesian decision rule and the comparison with conventional energy detection-based approaches is made on the basis of a theoretical analysis which generically models the noise as white Gaussian zero-mean process and analysis versus the SNR and in *Low-SNR Regime* are made by considering only such a kind of noise modeling.

In [19] the focus is on a Cooperative Spectrum Sensing (CCS) and a dynamic spectrum sensing cycle is proposed for reducing the effects of the overall system latency. The authors analyze the performance of the proposed solution by considering shadow faded communication channel and Montecarlo simulations to the proposed system modeling. Once again, the analytical extraction of the probability of detection is carried out by considering and additive white Gaussian noise in the energy detector hypothesis test.

In [20] the authors face the problem of the wideband spectrum sensing by also proposing some new performance metrics as the *probability of insufficient spectrum opportunity* and the *probability of excessive interference opportunity*. A deep analysis (both theoretical and numerical) is also carried out for comparing the behavior of different uniform sampling schemes (i.e. partial-band Nyquist sampling, sequential narrowband Nyquist sampling, and integer under-sampling) under different SNRs. In any case the non-ideality introduced by a real receiver chain are not dealt with.

In [21] the focus is on the spectrum sensing performance evaluation when multiple primary users are present in the operating scenario. Indeed, in such circumstances, due to the level of the aggregated interference caused by the multiple PUs, can generate a spatial false alarm (SFA) effect which in turn can reduce the SUs' medium access probability. Beyond the interesting interference model setup for taking into account the presence of multiple PUs, the proposed noise model considers a zero-mean additive white Gaussian noise (AWGN) with unit variance and the impact of channel non-ideality is analyzed only by considering the random fluctuations due to fading channels.

Finally, in [26] a two-step sensing method is presented and specifically tuned and setup for proposing an energy-effective solution. In particular, a two time-saving and energy efficient one-bit cooperative spectrum sensing (TSEEOB-CSS) is analyzed by considering several figures of merit as energy-efficiency, time-savings, probability of detection and probability of false alarms, for different values of thresholds used for the occupancy detection and at different SNRs. Compared with other solutions available in literature, the method shows very interesting performance also for  $\text{SNR} < 0$  dB, but the authors highlight as more research is needed for facing the problem of noise uncertainty and the need to derive closed-form expressions for other different parameters on the system performance.

Consequently, the above studies highlight that, even if an extensive performance analysis of spectrum sensing algorithms is available in literature, generally the effects of the non-ideality of a real receiver chain involved in common hardware devices

employed for CR implementation (i.e. SDR) is not adequately dealt with. As matter of fact, recent papers and standard draft [27], [7] remark how the performance of spectrum sensing methods are affected by the “noise uncertainty” (meant as not accurate knowledge of the noise variance) which is a parameter that strongly depends on the RX chain of real instruments. This paper includes also this aspect in the performance analysis by quantifying the effects due to the main stages involved in a real receiver chain.

### III. REAL INSTRUMENT RECEIVING CHAIN

Typical architecture of a commercial SDR is sketched in **Errore. L'origine riferimento non è stata trovata.** It is constituted by six main sections:

- 1) Antenna: employed for capturing the RF signal;
- 2) Low-noise amplifier: for increasing the system sensitivity;
- 3) Filter banks: to select (through suitable software-controlled multiplexer) a specific input frequency interval among ones available. This operation generally allows increasing the frequency selectivity;
- 4) Amplification and down-conversion for I/Q demodulation: the I and Q (base-band) components of the signal are extracted.
- 5) Analog-to-Digital conversion: I and Q components are sampled and quantized;
- 6) Data Processing: the acquired samples of I and Q component are processed with a suitable processing unit, typically a Digital Signal Processor (DSP) and/or a Field Port Programmable Array (FPGA). In some practical cases, on-board operating systems are available to manage all tasks.

The sections 1)-4) involved in the SDR receiver chain generally introduce noise and non-linearities on the input signal which result as a general SNR decreasing.

In addition, section 5) introduces further noise components mainly due to quantization processes, which could affect the final result provided by the processing stage (section 6).

As a consequence, the nominal performance of spectrum sensing methods and algorithms can be drastically reduced by the non-ideality of the measurement chain.

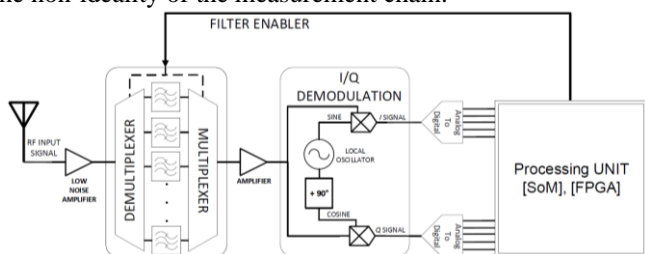


Figure 1. Block Diagram of an SDR Receiving Chain

### IV. ADOPTED TEST METHODOLOGY

To determine the influence of a real instrument receiving chain, the experimental tests have been organized according to a comparison methodology. In particular, a scenario consisting of an ATSC signaling user has been chosen as primary transmission over a specific 6 MHz channel and, to reveal its presence/absence, an energy detection scheme [16], [25] has been adopted. Such scenario has been simulated through MATLAB<sup>TM</sup> software, both in ideal conditions (machine double precision samples) and after an analog-to-digital

conversion stage by means of a 12-Effective-Number-of-Bits (ENOB)  $\Sigma$ - $\Delta$  converter model. Furthermore, the same signal has been generated by a vector signal generator and acquired through a software defined radio, having as A/D conversion stage equivalent to the  $\Sigma$ - $\Delta$  converter modeled by MATLAB in simulation environment. Actually, such kind of converters are quite common in SDRs and they are also deeply studied in literature [28]. Both scenarios, deriving from simulation and real hardware acquisition, have been processed by the same spectrum sensing algorithm (to avoid algorithm unpredictable behavior, the acquired samples from SDRs have also been processed by the MATLAB software) and results are reported in this work. The power of ATSC signal has been suitably set to obtain several Signal-to-Noise ratios. Performance achievements are provided through typical Key Performance Indicators (KPIs) in detection theory, such as Probability of Detection ( $P_d$ ) and Probability of False Alarm ( $P_{fa}$ ).

#### A. Noise behavior characterization of SDR

Unlike simulation environment, where noise can be shaped and distributed quite easily using suitable mathematical functions, when SDRs are adopted to acquire and process signals, their noise contribution must be accurately evaluated. The motivation to characterize their noise levels is twofold: firstly, it gives an indication of the minimum of level of signal power that allows to distinguish it from the noise; secondly, it can be used to control SNR values when testing an algorithm on such devices. To achieve the goal, the SDR Noise Figure (NF) and the average noise power level in the channel of interest have been evaluated as follows:

- The antenna port has been terminated with a matched 50  $\Omega$  load and the Display Averaged Noise Level (DANL) has been evaluated;
- the thermal noise has been computed by monitoring the environment temperature during acquisition time by using a thermometer.
- The difference between the obtained quantities (in dB) has provided the NF result.

#### B. The developed laboratory set-up

To acquire data from real hardware, a suitable laboratory test set-up has been developed and it is shown in **Errore. L'origine riferimento non è stata trovata.** It is composed of:

- a vector signal generator, namely Agilent N5182A MXG, capable to play several waveform typologies, among which ATSC signals needed to our purpose;

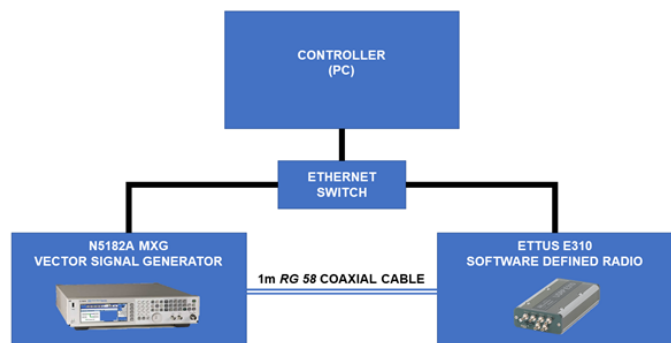


Figure 2. Block diagram of the laboratory set-up

- a software defined radio, namely Ettus E310 [29], having two independent TX/RX chains and capable to transmit/receive data in frequency interval spanning from 70 MHz to 6 GHz, with an instantaneous bandwidth up to 56 MHz;
- a 1-m-long coaxial cable, RG 58 category, used to connect generator and SDR (the use of cable instead of an antenna has been considered to isolate the effect of non-idealities to the instrument itself and consider a controlled transmission cable, where attenuation is a straightforward parameter to be evaluated);
- one PC, used as controller, able to configure and start the data streaming from VSG and to manage data acquisition by SDR.
- an ethernet switch, used to connect all involved device to the same subnetwork.

The operations are executed in the following order:

- the controller sends signal parameters to VSG and enable continuous streaming from its RF output port;
- the controller enables SDR data acquisition from its antenna port;
- processed data are then returned to the controller for performance evaluation.

### C. SNR setting for SDR acquisition

To obtain wanted Signal-to-Noise ratios for signals acquired by the SDR device, several operations are needed.

1. Noise Level (DANL) computation for the device under test (as stated in subsection IV.A);
2. Evaluation of the attenuation due to coaxial cable ( $Att$ );
3. Evaluation of the mathematical relation between imposed and actual TX power for the VSG (Correction Factor  $C$ );
4. Imposition of a specific power level to the VSG through a command by the controller ( $P_{imp}$ ):

$$P_{imp}(dBm) = DANL_{dBm} + SNR_{dB} + Att_{dB} + C_{dB} \quad (1)$$

Bullets 2. and 3. have been accomplished by using a reference power meter (Keysight N1911A), thus measuring the power at VSG RF output port and at the opposite edge of the coaxial cable.

## V. PERFORMANCE ASSESSMENT

### A. Preliminary characterization results

The characterization methodology reported in Section IV has led to the following results:

- $DANL_{dBm} = -89.84 \text{ dBm}$
- Thermal Noise at  $27^\circ \text{C}$ :  $W_{Th} = -97.02 \text{ dBm}$ , by considering a  $T = 300 \text{ K}$  and  $B = 48 \text{ MHz}$ , as acquisition bandwidth;
- Noise Figure (NF):  $NF = DANL - W_{Th} = 7.18 \text{ dB}$ ;
- Cable attenuation (at 600 MHz frequency):  $0.7 \text{ dB}$ ;
- Mathematical relation between imposed and generated power at VSG RF output port:

$$P_{gen,dBm} = 1.04P_{in,dBm} + 0.123 \quad (2)$$

### B. Test scenario parameters

The characterization results reported in subsection V.A has allowed to replicate the wanted channel and signal conditions also in real acquisition case. In Table , a correspondence between required SNR and the power level to be imposed to VSG is reported. In this work, SNRs ranging from -15 dB to 5 dB have been adopted. The motivation for the high level of detail in negative SNR case is due to the results outcome.

Scenario parameters are described in Table . In particular, considering the American ATSC standard, 8 different 6 MHz channels have been chosen and primary transmission has been activated on channel 4 (corresponding to 35 in official channel list).

Furthermore, the number of acquisitions for each test condition (in terms of SNR) has been set to 10000, in order to correctly estimate  $P_d$  and  $P_{fa}$  values according to frequentist approach, applying the empirical rule that the product of the smallest probability to be estimated and the number of tests should approach  $10^2$ .

Table I. Simulation parameters for tested scenario

Frequency Interval [MHz]	Number of Channels	Channel Bandwidth [MHz]	Occupied Channel Number	Acquisition number
578 – 626	8 (32-39)	6	35	10000

Table II. Correspondence between SNR and imposed power ( $P_{imp}$ )

SNR [dB]	$P_{imp}$ [dBm]
-15	-100.36
-10	-95.54
-9	-94.57
-8	-93.61
-7	-92.64
-6	-91.68
-5	-90.71
0	-85.88
5	-81.07

### C. Figures of Merit Definition

The definition of the adopted figures of merit according to frequentist approach is reported in this paragraph.

In particular:

- Probability of Detection ( $P_d$ ):

$$P_d = \frac{1}{N_{test}} \sum_{i=1}^{N_{test}} (E_i > Th|H_1) \quad (3)$$

- Probability of False Alarm ( $P_{fa}$ ):

$$P_{fa} = \frac{1}{N_{test}} \sum_{i=1}^{N_{test}} (E_i > Th|H_0) \quad (4)$$

In Eqs. 3, 4 the following notation has been used:

- $N_{test}$ , total number of acquisitions for a specific test condition (i.e.  $10^4$ );

- $E_i$ , energy measured in the  $i_{th}$  test for the channel under test;
- $H_1$  and  $H_0$  are binary hypotheses denoting occupied and free channel, respectively;
- $Th$  is the energy threshold, due to imposed false alarm rate.

D. Set-up calibration

Before testing the algorithm on the chosen scenario, a calibration phase has been carried out to find the threshold value empirically.

In particular, both in simulation and laboratory environments, a surely vacant channel has been acquired for a long period of time, by acquiring the same number of channel content time records than the one used in test phase.

As a design parameter, values for acceptable  $P_{fa}$  range in the [1-10] % interval.

Therefore, energy detection has been applied to the considered vacant channel by testing a large number of possible thresholds, taking into account the number of false positives (FPs), i.e. tests where the current threshold value was passed, although only noise samples were acquired. Through a normalization process, FPs have been transformed into estimated  $P_{fa}$ s, and threshold values allowing to obtain target  $P_{fa}$ s have been stored and used for the test phase.

This procedure has been adopted for two reasons:

- No white Gaussian assumptions about noise distribution after quantization process seem reasonable;
- Acquired data from SDR device and data used in simulation environment are independent and noise realizations could have different distributions; SNR, quantization process and signal type are the only common and controlled parameters.

E. Obtained Performance in non-quantization case

First tests have been carried out in ideal case, where data were generated by means of a MATLAB™ software and no further quantization process was applied to samples. This is necessary to have a performance benchmark and to assess the suitability of the calibration procedure for threshold choice.

Firstly, the relation between imposed  $P_{fa}$  and obtained one is provided for a vacant channel during test phase. As described in the subsection V.B, channels 32-34 and 36-39 were intentionally left vacant during test phase. In **Errore. L'origine riferimento non è stata trovata.**

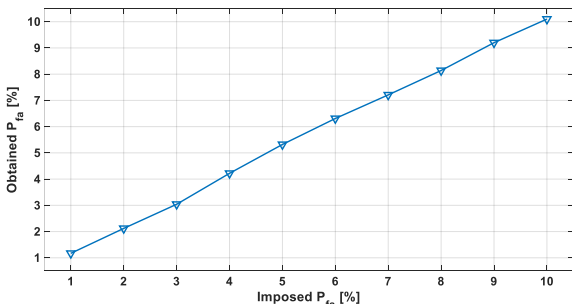


Figure 3.  $P_{fa}$  verification during test phase in vacant channel.

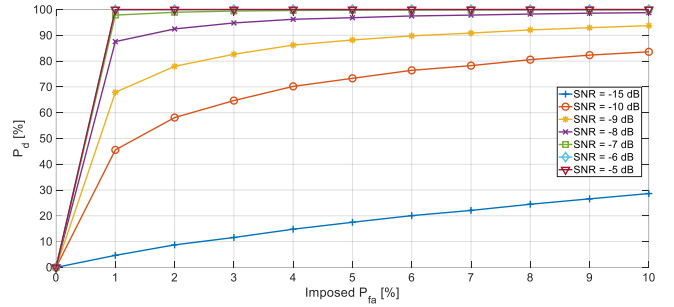


Figure 4. ROC curve for ideal case.  $P_d$  vs imposed  $P_{fa}$  in percentage values

**riferimento non è stata trovata.** the maximum  $P_{fa}$  values among all vacant channels are reported.

As **Errore. L'origine riferimento non è stata trovata.** reports, obtained values are aligned with the imposed one and, in the worst case, the obtained  $P_{fa}$  value is 17% greater than the imposed one (1.17% vs 1%). This proves that the choice of finding an empirical threshold to warrant controlled  $P_{fa}$  is reasonable.

In terms of obtained  $P_d$ s for the ideal case, results are reported in **Errore. L'origine riferimento non è stata trovata.** Result presentation is given by ROC curves. The capability to correctly detect the signal when present is increasing with SNR values and a  $P_d \geq 90\%$  (usually denoted as acceptable lower bound) is ensured for  $SNR \geq -8$  dB. Transmitted signal is always corrected revealed ( $P_d = 100\%$ ) when  $SNR \geq -7$  dB. Although evaluated, cases of  $SNR > -5$  dB are not reported in the figure for clarity reasons, since they behave as  $SNR = -5$  dB, due to the  $P_d$  increasing trend with SNR.

F. Obtained Performance in 12-bit quantization case in simulation environment

When a  $\Sigma$ - $\Delta$  analog-to-digital conversion is applied to original samples, it was expected a slight behavior on the obtained performance, due to the addition of quantization noise to the original signal-to-noise ratio. As proved in [30], quantization process can be considered, in energy domain, as a further noise source, whose quantification depends on the typology of adopted quantizer.

Actually,  $\Sigma$ - $\Delta$  converter is considered one of the best methods in terms of noise contribution, due to its intrinsic capability to reduce and “shape” quantization noise. In any case, due to the hardware design parameters of the SDR under test, we decided

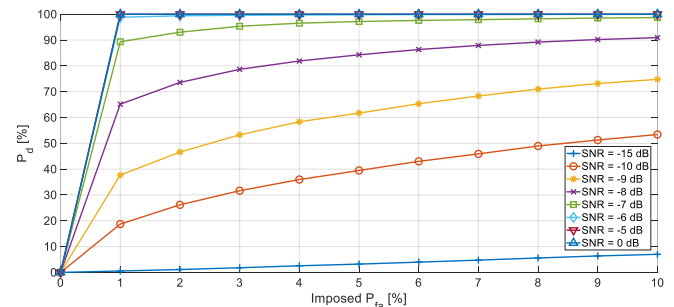


Figure 5. ROC curve for quantization case in simulation.  $P_d$  vs imposed  $P_{fa}$  in percentage values

Table III. Comparison of  $P_d$  values in simulation environment - ideal vs quantization cases

SNR [dB]	$P_d$ [%] ideal case	$P_d$ [%] quantization
-15	17.5	3.2
-10	73.3	39.5
-9	88.2	61.7
-8	96.8	84.3
-7	99.7	97.2
-6	100	99.8

to adopt this digital conversion stage to make the spectrum sensing method work under the same operating conditions.

As **Errore. L'origine riferimento non è stata trovata.** shows ROC curves, deriving from the application of sensing scheme to quantized data, show a degradation in performance, if compared to Figure 4**Errore. L'origine riferimento non è stata trovata.**, that strictly depends on the SNR.

Considering a fixed  $P_{fa}$  value (e.g. 5%), in Table III, a comparison is shown in terms of obtained performance for different SNR conditions.

The trend is similar for all considered  $P_{fa}$ s, and it remarks an important degradation after the application of quantization. In particular, for SNRs lower than -7 dB, we have relative loss ranging from 13% to 46% down to -10 dB. Obtained results at SNR = -15 dB, regarding quantization case, cannot be evaluated since  $P_d$  is lower than the imposed  $P_{fa}$ , meaning that the sensing algorithm is declaring the channel under test as free. In ideal case, also SNR = -15 dB allows to have detection, although with a low  $P_d$  value.

### G. Obtained Performance with SDR acquisition

SDR acquisition has been carried out after the characterization phase and taking into account the estimated parameters. Results are depicted in **Errore. L'origine riferimento non è stata trovata.**

Unlike results in simulation environment, the performance gap between SNR = -15 dB and SNR = -10 dB is less evident. In particular, performance results remain low and are uniformly increasing with SNR. Acceptable values ( $P_d > 90\%$ ) are obtained for  $SNR \geq -5$  dB, while it happened at  $SNR \geq -7$  dB in simulation case. Furthermore, results with SDR show an additional degradation step with respect to quantization case, thus confirming the initial claim of this paper, i.e. *how nominal Signal-to-Noise ratio is not sufficient to model the impairments of a real acquisition, even jointly with a modeling of the*

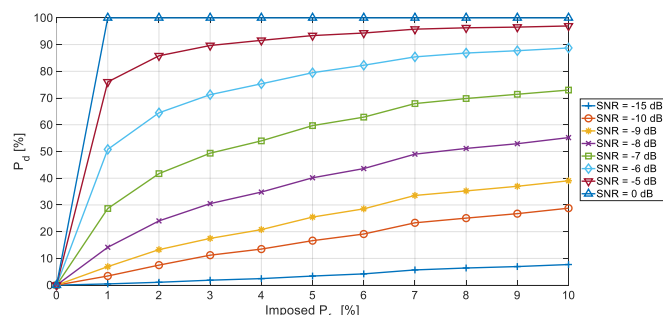


Figure 6. ROC curve for SDR processing case.  $P_d$  vs imposed  $P_{fa}$  in percentage values

digitalization process. In Table IV, detection probability values are reported for  $P_{fa} = 5\%$  and compared with those obtained in simulation case. The claim is particularly true for lower SNRs, where performance worsening is quite critical.

Table IV. Comparison of  $P_d$  values in all tested situations.

SNR [dB]	$P_d$ [%] ideal	$P_d$ [%] quantization	$P_d$ [%] SDR
-15	17.5	3.2	3.4
-10	73.3	39.5	16.6
-9	88.2	61.7	25.5
-8	96.8	84.3	40.2
-7	99.7	97.2	59.7
-6	100	99.8	79.5
-5	100	100	93.4

## VI. CONCLUSION

In this paper a metrological approach has been proposed to prove the effect of a real instrument RX-chain on the performance of a widely known spectrum sensing approach, i.e. energy detection. Results in terms of ROC curves clearly show the worsening of the performance, beyond the simple effect of the SNR, that is the main parameter adopted to assess goodness of a novel algorithm of spectral occupancy detection. Results are further enforced by a preliminary characterization of noise behavior of the device under test and the application of a methodology to apply the correct SNR in real acquisition process and to model, in simulation environment, the digitalization process.

## REFERENCES

- [1] W. Wang, "Collaborative Multimedia Source-Protocol Coordination: A Cross-Layer QoE Study in Modern Wireless Networks," IEEE Systems Journal, vol. PP, no. 99, pp. 1–7, 2017.
- [2] S. T. F. Al-Janabi and D. K. H. Ghareeb, "Real-life enhancement of QoE for social network applications," in 2017 Annual Conf. on New Trends in ICT Applications (NTICT), March 2017, pp. 63–68.
- [3] FCC, "Spectrum Policy Task Force Report, ET Docket No. 02-135," Tech. Rep., 2011.
- [4] T. Taher, R. Attard, A. Riaz, D. Roberson, J. Taylor, K. Zdunek, J. Hallio, R. Ekman, J. Paavola, J. Suutala, J. Roning, M. Matinmikko, M. Hyty, and A. MacKenzie, "Global spectrum observatory network setup and initial findings," in 2014 9th Int. Conf. on Cognitive Radio Oriented Wireless Net. and Commun. (CROWNCOM), June 2014, pp. 79–88.
- [5] L. Angrisani, D. Capriglione, L. Ferrigno, and G. Miele, "Frequency agility in cognitive radios: A new measurement algorithm for optimal operative frequency selection," *Measurement*, vol. 82, pp. 26–36, 2016.
- [6] M. Song, C. Xin, Y. Zhao, and X. Cheng, "Dynamic spectrum access: from cognitive radio to network radio," *IEEE Wireless Communications*, vol. 19, no. 1, pp. 23–29, February 2012.
- [7] "IEEE Standard for Information technology– Local and metropolitan area networks– Specific requirements– Part

- 22: Cognitive Wireless RAN Medium Access Control (MAC) and Physical Layer (PHY) specifications: Policies and procedures for operation in the TV Bands,” IEEE Std 802.22-2011, pp. 1–680, July 2011.
- [8] J. Mitola and G. Q. Maguire, “Cognitive radio: making software radios more personal,” IEEE Pers. Commun., vol. 6, no. 4, pp. 13–18, Aug 1999.
- [9] L. Gonzales-Fuentes, K. Barbé, W. Van Moer, N. Björnsell, Cognitive Radios: Discriminant Analysis for Automatic Signal Detection in Measured Power Spectra, IEEE Transactions on Instrumentation and Measurement, Vol. 62, Issue 12, 2013, pp. 3351-3360.
- [10] L. Angrisani, D. Capriglione, G. Cerro, L. Ferrigno, and G. Miele, “Employment of software defined radios for dual-use in distributed spectrum monitoring system,” in 2016 IEEE 2nd Int. Forum on Res. and Tech. for Society and Industry (RTSI), Sept 2016, pp. 1–5.
- [11] D. Bao, L. De Vito, S. Rapuano, “A Histogram-Based Segmentation Method for Wideband Spectrum Sensing in Cognitive Radios”, IEEE Transactions on Instrumentation and Measurement, Vol.62, Issue 7, 2013, pp. 1900 – 1908.
- [12] P. Ferrari, A. Flammini, E. Sisinni, “New Architecture for a Wireless Smart Sensor Based on a Software-Defined Radio”, IEEE Transactions on Instrumentation and Measurement, vol. 60, issue 6, 2011, pp. 2133 – 2141.
- [13] M. Hamid, N. Björnsell, W. Van Moer, K. Barbé, S. Ben Slimane, “Blind Spectrum Sensing for Cognitive Radios Using Discriminant Analysis: A Novel Approach”, IEEE Transactions on Instrumentation and Measurement, vol. 62, issue 11, 2013, pp. 2912 – 2921.
- [14] W. A. Jerjawi, Y. A. Eldemerdash, O. A. Dobre, “Second-Order Cyclostationarity-Based Detection of LTE SC-FDMA Signals for Cognitive Radio Systems”, IEEE Transactions on Instrumentation and Measurement, vol. 64, issue 3, 2015, pp. 823 – 833.
- [15] S. Yarkan, “A Generic Measurement Setup for Implementation and Performance Evaluation of Spectrum Sensing Techniques: Indoor Environments”, IEEE Transactions on Instrumentation and Measurement, vol. 64, issue 3, 2015, pp. 606 – 614.
- [16] H. Urkowitz, "Energy detection of unknown deterministic signals," in Proceedings of the IEEE, vol. 55, no. 4, pp. 523-531, April 1967. doi: 10.1109/PROC.1967.5573
- [17] R. Fantacci and A. Tani, “Performance Evaluation of a Spectrum-Sensing Technique for Cognitive Radio Applications in B-VHF Communication Systems,” IEEE Trans. on Vehicular Technology, vol. 58, no. 4, pp. 1722–1730, May 2009.
- [18] J. Y. Wu, C. H. Wang, and T. Y. Wang, “Performance Analysis of Energy Detection Based Spectrum Sensing with Unknown Primary Signal Arrival Time,” IEEE Trans. Commun., vol. 59, no. 7, pp. 1779–1784, Jul. 2011.
- [19] Q. Wang, D. W. Yue, and F. C. M. Lau, “Performance of cooperative spectrum sensing over fading channels with low signal-to-noise ratio,” IET Communications, vol. 6, no. 13, pp. 1988–1999, Sept. 2012.
- [20] Z. Sun and J. N. Laneman, “Performance Metrics, Sampling Schemes, and Detection Algorithms for Wideband Spectrum Sensing,” IEEE Trans. Sig. Process., vol. 62, no. 19, pp. 5107–5118, Oct 2014.
- [21] A. Furtado, L. Irio, R. Oliveira, L. Bernardo, and R. Dinis, “Spectrum Sensing Performance in Cognitive Radio Networks With Multiple Primary Users,” IEEE Trans. on Vehicular Technology, vol. 65, no. 3, pp. 1564–1574, Mar. 2016.
- [22] E. Rebeiz, A. S. H. Ghadam, M. Valkama, and D. Cabric, “Spectrum Sensing Under RF Non-Linearities: Performance Analysis and DSP-Enhanced Receivers”, IEEE Trans. on Sig. Proc., vol. 63, no. 8, Apr. 15, 2015, pp. 1950-1964.
- [23] D. Capriglione, G. Cerro, L. Ferrigno and G. Miele, "The effect of ADC vertical resolution on the performance of an energy detection algorithm in cognitive radios," 2018 IEEE International Instrumentation and Measurement Technology Conference (I2MTC), Houston, TX, USA, 2018, pp. 1-6. Doi: 10.1109/I2MTC.2018.8409825.
- [24] G. Betta, L. Ferrigno, M. Laracca, “Cost-Effective FPGA instrument for harmonic and interharmonic monitoring”, IEEE Transactions on Instrumentation and Measurement, Vol. 62, Issue 8, pp. 2161-2170, DOI 10.1109/TIM.2013.2264862, 2013.
- [25] L. Angrisani, D. Capriglione, G. Cerro, L. Ferrigno, and G. Miele, “A dual step energy detection-based spectrum sensing algorithm for cognitive vehicular ad hoc networks,” in 2015 IEEE I2MTC Proceedings, May 2015, pp. 1622–1627.
- [26] Zhao, Nan, Yu, Fei Richard Sun, Hongjian Nallanathan, Arumugam, “Energy-efficient cooperative spectrum sensing schemes for cognitive radio networks”, EURASIP Journal on Wireless Communications and Networking, 2013. Doi: 10.1186/1687-1499-2013-120.
- [27] S. J. Shellhammer, "Spectrum Sensing in IEEE 802.22", IAPR Wksp. Cognitive Info. Processing, 2008-June.
- [28] A. Morgado, R. del Rio, J. M. dela Rosa, “High-Efficiency Cascade  $\Sigma\Delta$  Modulators for the Next Generation Software-Defined-Radio Mobile Systems”, IEEE Transactions on Instrumentation and Measurement, vol. 61, issue 11, 2012, pp. 2860 – 2869.
- [29] Ettus Research, E310 SDR platform, online at: [ettus.com/content/files/USRP\\_E310\\_Datasheet.pdf](http://ettus.com/content/files/USRP_E310_Datasheet.pdf).
- [30] D. Marco and D. L. Neuhoff, "The Validity of the Additive Noise Model for Uniform Scalar Quantizers", IEEE Transactions on Information Theory, Vol. IT-51, No. 5, pp. 1739–1755, May 2005. doi:10.1109/TIT.2005.846397